HHS Public Access

Author manuscript

Circ Res. Author manuscript; available in PMC 2021 September 17.

Published in final edited form as:

Circ Res. 2020 January 17; 126(2): 182–196. doi:10.1161/CIRCRESAHA.119.315483.

Metabolic Remodeling Promotes Cardiac Hypertrophy by Directing Glucose to Aspartate Biosynthesis

Julia Ritterhoff, **Sara Young**, **Outi Villet**, **Dan Shao**, **F. Carnevale Neto**, **Lisa F. Bettcher**, **Yun-Wei A. Hsu**, **Stephen C. Kolwicz Jr**, **Daniel Raftery**, **Rong Tian**

Department of Anesthesiology and Pain Medicine (J.R., S.Y., O.V., D.S., Y.-W.A.H., S.C.K., R.T.) and Department of Anesthesiology and Pain Medicine, Northwest Metabolomics Research Center (F.C.N., L.F.B., D.R.), Mitochondria and Metabolism Center, University of Washington, Seattle.

Abstract

RATIONALE: Hypertrophied hearts switch from mainly using fatty acids (FAs) to an increased reliance on glucose for energy production. It has been shown that preserving FA oxidation (FAO) prevents the pathological shift of substrate preference, preserves cardiac function and energetics, and reduces cardiomyocyte hypertrophy during cardiac stresses. However, it remains elusive whether substrate metabolism regulates cardiomyocyte hypertrophy directly or via a secondary effect of improving cardiac energetics.

OBJECTIVE: The goal of this study was to determine the mechanisms of how preservation of FAO prevents the hypertrophic growth of cardiomyocytes.

METHODS AND RESULTS: We cultured adult rat cardiomyocytes in a medium containing glucose and mixed-chain FAs and induced pathological hypertrophy by phenylephrine. Phenylephrine-induced hypertrophy was associated with increased glucose consumption and higher intracellular aspartate levels, resulting in increased synthesis of nucleotides, RNA, and proteins. These changes could be prevented by increasing FAO via deletion of ACC2 (acetyl-CoA-carboxylase 2) in phenylephrine-stimulated cardiomyocytes and in pressure overload–induced cardiac hypertrophy in vivo. Furthermore, aspartate supplementation was sufficient to reverse the antihypertrophic effect of ACC2 deletion demonstrating a causal role of elevated aspartate level in cardiomyocyte hypertrophy. 15N and 13C stable isotope tracing revealed that glucose but not glutamine contributed to increased biosynthesis of aspartate, which supplied nitrogen for nucleotide synthesis during cardiomyocyte hypertrophy.

CONCLUSIONS: Our data show that increased glucose consumption is required to support aspartate synthesis that drives the increase of biomass during cardiac hypertrophy. Preservation

Correspondence to: Rong Tian, MD, PhD, Mitochondria and Metabolism Center, University of Washington School of Medicine, 850 Republican St, Seattle, WA 98109. rongtian@u.washington.edu.

Author Contribution

J. Ritterhoff and R. Tian designed experiments and wrote the manuscript. J. Ritterhoff, S. Young, O. Villet, D. Shao, F.C. Neto, and L.F. Bettcher performed experiments, and J. Ritterhoff analyzed the data. Y.-W.A. Hsu provided help with animal experiments. S.C. Kolwicz provided critical advice during study design. R. Tian and D. Raftery supervised the project.

The online-only Data Supplement is available with this article at https://www.ahajournals.org/doi/suppl/10.1161/CIRCRESAHA.119.315483.

Disclosures

None.

of FAO prevents the shift of metabolic flux into the anabolic pathway and maintains catabolic metabolism for energy production, thus preventing cardiac hypertrophy and improving myocardial energetics.

VISUAL OVERVIEW: An online visual overview is available for this article.

Keywords

aspartic acid; cardiomyocyte; glucose; hypertrophy; metabolism; nucleotides

An important element of pathological remodeling of the heart is the development of cardiac hypertrophy, characterized by an enlargement of individual cardiomyocytes. Although the hypertrophic growth of cardiomyocytes provides short-term benefits, for example, reduces wall stress and sustains cardiac function, it becomes maladaptive and predisposes to heart failure in the long term.[1,2] Cardiac metabolism changes early during the development of cardiac hypertrophy. It is characterized by a shift in fuel metabolism away from fatty acid oxidation (FAO) to an increased reliance on glucose, followed by an overall reduction in oxidative metabolism.[3–5] Previous research has shown that increasing the oxidation of either glucose or fatty acids (FAs) could improve myocardial energetics and contractile function of the hypertrophied hearts.[6–10] However, increasing glucose utilization did not reduce cardiac hypertrophy despite improvement of cardiac energetics. These observations corroborate recent work showing that increased intracellular glucose, apart from serving as an energy source, stimulates pro-growth signaling pathways.[11–13] On the contrary, we have previously shown that cardiac-specific deletion of ACC2 (acetyl-CoA carboxylase 2) in vivo preserves FAO during pathological stress, such as pressure overload and angiotensin II infusion, and protects the hearts against cardiomyocyte hypertrophy.[8,14] It remains unclear, however, whether FAO directly regulates hypertrophic growth or whether the attenuation of hypertrophy is a consequence of improved myocardial energetics and function when FAO is preserved.

The tricarboxylic acid (TCA) cycle is a central hub that integrates catabolic and anabolic pathways.[15] While oxidation of acetyl-CoA to CO_2 is the primary function of the TCA cycle in energy metabolism, the TCA cycle also provides metabolites for biosynthesis of glucose, FAs, and amino acids, especially in proliferating cells. In cancer cells, carbon substrates such as glutamine are converted into cellular building blocks via the TCA cycle to support biomass synthesis and cell duplication instead of being used for ATP generation.[16–19] On the contrary, as the energy demand for cardiac contraction is high while the biosynthetic demand is low for the nonproliferative cardiomyocyte, majority of carbon fluxes in cardiac metabolism are directed toward energy production. Thus far, most studies of cardiac metabolism have focused on the catabolic reactions for energy provision except for a few studies on the anabolic role of glycolytic pathway in cardiac hypertrophy.[20,21] Moreover, little is known about the role of the TCA cycle in regulating the growth of cardiomyocytes.

In this study, we tested the hypothesis that metabolic reprogramming during cardiac hypertrophy remodels the TCA cycle toward anabolic metabolism to support increased biomass synthesis. We show that the metabolic switch from FAs to glucose is

associated with an increase in anabolic metabolism, which provides glucose-derived aspartate for cellular hypertrophy. Furthermore, preservation of FAO reduces anabolic substrate availability and prevents cardiomyocyte hypertrophy. Taken together, our data unveil a previously unrecognized contribution of substrate switch to cellular growth in nonproliferating tissue and identify a target for antihypertrophic intervention.

METHODS

The data that support the findings of this study are available from the corresponding author on reasonable request.

A detailed description of Materials and Methods is available in the Online Data Supplement.

Animal Studies

All protocols concerning animal studies were approved by the Institutional Animal Care and Use Committee at the University of Washington. All personnel were blinded during animal experiments (surgery, echocardiography, tissue harvest). ACC2 flox/flox MCM (MerCreMer) mice were bred on a C57BL6 background as described previously.[14,22] Male 10- to 12-week-old mice weighing 22 to 28 g underwent transverse aortic constriction (TAC) or sham surgery as described previously.[23] Echocardiography in anesthetized mice was performed as described previously.[13] Primary end points for the in vivo study were myocardial aspartate levels and ^{13}C in vivo labeling. For detailed information, see Materials and Methods in the Online Data Supplement.

Long-Chain FA Mix Preparation

FA-BSA stock was prepared at a final concentration of 5 mmol/L FA with 12% FA-free BSA (molecular ratio, 2.2:1; both purchased from Sigma-Aldrich) in glucose/pyruvate-free Krebs-Henseleit buffer with modifications as described previously.[24] The following long-chain FAs (in percentage from molecular weight) were used: palmitic acid 50.9, palmitoleic acid 10.8, linoleic acid 13.2, linolenic acid 0.3, oleic acid 23.6, and stearic acid 1.2. Final concentration of FA used in experiments was 0.4 mmol/L. For detailed information, see Materials and Methods in the Online Data Supplement.

Construction and Purification of Adenoviral Expression Vectors

Recombinant adenoviruses were generated using homologous recombination in HEK293 (human embryonic kidney 293) cells as described before.[13,25] For detailed information, see Materials and Methods in the Online Data Supplement.

Adult Cardiomyocyte Isolation and Culture

Primary adult cardiomyocytes (ACMs) were isolated from male Wistar rats (200–250 g) following a standard enzymatic digestion protocol as described before.[26] After an adhesion period of 1 hour, cardiomyocytes were cultured in Medium 199 (Sigma-Aldrich; glucose medium) and transduced with indicated adenoviruses (shScr or shACC2, day 0). Medium was changed to glucose+FA (glc+FA) medium (5.5 mmol/L glucose, 0.4 mmol/L FA, 0.1 mU/mL insulin) on day 1. On day 2, ACMs were stimulated with 10 μmol/L phenylephrine

(PE) for another 24 hours before harvest for different assays on day 3. For detailed information, see Materials and Methods in the Online Data Supplement.

For quantification of cell size under different conditions, ACMs were treated 2 hours with dichloroacetate (5 μmol/L), etomoxir (200 μmol/L), or nucleotide precursor mix (100 μmol/L hypoxanthine, adenine, and guanine, 50 μmol/L thy-mine, 200 μmol/L uridine) before addition of PE for 24 hours. LacZ/Glut1 (β-galactosidase/glucose transporter 1) adenoviral overexpression (MOI 5), supplementation with aspartate (10 mmol/L)/dimethyl-aspartate (DM-asp; 1 mmol/L), or glutamine (10 mmol/L) was performed 24 hours before PE stimulation. Pyruvate (11 mmol/L) was replaced for glucose 24 hours before PE stimulation. All chemicals were purchased from Sigma-Aldrich.

Quantification of Cell Size

Cells—Twenty-four hours after PE stimulation, bright-field images of ACMs were taken with a Nikon Eclipse TS100 microscope and attached camera. Length and width of individual cardiomyocytes were quantified by ImageJ software (National Institutes of Health) and cell size depicted as width/length ratio. Two images per condition and ≈15 cells/image were analyzed for each condition.

In Vivo—Two weeks post-TAC, mouse heart tissues were rinsed with PBS and fixed in 10% neutral buffered formalin. Sample processing and staining were performed by the Histology and Imaging Core at the University of Washington. Slides were stained with Wheat Germ Agglutinin to measure cell size. Fluorescence images were acquired by confocal microscopy (Nikon).

Measurement of Intracellular ATP Levels and Cell Viability

For detailed information, see Materials and Methods in the Online Data Supplement.

Glucose Uptake

ACMs were plated on glass-bottom fluorodishes (World Precision Instruments) and incubated with 2-NBDG (2-(*N*-(7-nitrobenz-2-oxa-1,3-diazol-4-yl)amino)-2-deoxyglucose; 300 μM; Life Technology) in glucose-free DMEM (Life Technology) for 90 minutes at 37°C in the dark. After washing off excessive fluorescent dye, intracellular fluorescence was acquired by confocal microscopy (Nikon). Subsequently. the images were quantified by ImageJ software (National Institutes of Health). Three images per condition and ≈10 cells/images were analyzed for each condition.

Glucose Consumption

Culture medium was collected at the end of experiments and stored at −80°C until analyses. Glucose concentration in the medium was measured with glucose test strips (Bayer Contour blood glucose test strips and meter). Glucose consumption was calculated based on a cell-free medium control and normalized to protein concentration.

Protein Synthesis

Protein synthesis was measured using the nonradioactive Surface Sensing of Translation assay as described previously with modifications.[27] For detailed information, see Materials and Methods in the Online Data Supplement.

RNA Synthesis

RNA synthesis was measured as described previously with modifications.[28] For detailed information, see Materials and Methods in the Online Data Supplement.

Stable Isotope Tracing

Cells—For isotope tracing experiments, ACMs were cultured in glc+FA medium and stimulated with PE for 24 hours as described above. For each condition, 0.2 to 0.5 million cells were used. Nonlabeled substrates were replaced with either $^{13}C_6$ glucose (5.5 mmol/L, CLM-1396; Cambridge Isotope Laboratories, Inc), U-^{13}C FA mix (0.4 mmol/L, 487937; Sigma-Aldrich), or $^{13}C_5$ glutamine (3.4 mmol/L, CLM-1822-H; Cambridge Isotope Laboratories, Inc) before the end of PE stimulation for 3 hours before metabolite extraction. For ^{15}N-aspartate labeling experiments, 10 mmol/L ^{15}N-aspartic acid (NLM-718–0.5; Cambridge Isotope Laboratories, Inc) was added to ACM at the same time than PE for 24 hours.

In Vivo—One week after sham/TAC surgery, mice were fasted for 4 hours before low-dose (1.5%) anesthesia with isoflurane. After 5 minutes, mice were injected with 1 mg/g body weight $^{13}C_6$ glucose (CLM-1396; Cambridge Isotope Laboratories, Inc) in saline. After 20 minutes, ventricles were excised, briefly washed in ice-cold PBS, and freeze-clamped in liquid nitrogen. The tissue freezing process took <5 seconds.

Metabolite Extraction and Mass Spectrometry

For detailed information, see Materials and Methods in the Online Data Supplement.

RNA Isolation, Real-Time Polymerase Chain Reaction, and Immunoblots

For detailed information, see Materials and Methods in the Online Data Supplement.

Statistics

The numbers of independent experiments are specified in the relevant figure legends. Data are expressed as mean+SEM. Statistical analysis was performed with Prism 7.0 or 8.0 software (GraphPad). Normal distribution of data was confirmed by Shapiro-Wilk test. Statistical comparisons between 2 groups were conducted by unpaired, 2-tailed *t* test. Statistical comparisons between ≥3 groups were conducted by 1-way ANOVA followed by a Tukey post hoc analysis to determine statistical significance. Linear regression in Online Figure IXC was performed using Prism 8. The value of $P<0.05$ was considered statistically significant. Heat maps were generated using MetaboAnalyst 4.0.[29] Peak intensities from GC/MS (gas chromatography–mass spectrometry) experiments were normalized and log transformed.

RESULTS

ACC2 KD in Cultured ACMs Increases FAO and Prevents Hypertrophy

To address the question whether FAO directly regulates hypertrophic growth of cardiomyocytes, we chose to investigate the pathological hypertrophy of ACMs in culture, where the influence of contraction and its related energy consumption is avoided. To decipher the role of substrate selection, ACMs were supplied with glucose (5.5 mmol/L) and mixed long-chain FAs (0.4 mmol/L), which we routinely use for perfused heart experiments.[8] ACMs cultured under this condition (glc+FA) did not show any morphological changes or any sign of lipotoxicity or cell death compared with ACMs cultured in conventional glucose medium (Online Figure IA and IB). We then knocked down ACC2 (ACC2 KD) by adenoviral shRNA delivery (shACC2) to study the effect of elevated FAO on cardiomyocyte hypertrophy (Figure 1A and 1B; Online Figure IC).

PE stimulation resulted in a 40% increase in cell size in glucose medium, as well as in glc+FA medium (Online Figure ID), indicating that FA supplementation per se is not sufficient to alter the growth of ACMs. However, ACC2 KD prevented hypertrophy of ACMs cultured in glc+FA medium (Figure 1C through 1F). Attenuation of hypertrophy correlated with elevated levels of FAO after ACC2 KD (Figure 1F and 1G). Inhibition of mitochondrial FAO with etomoxir reversed the protective effect of ACC2 deletion on ACM hypertrophy, demonstrating its dependence on mitochondrial FAO (Figure 1D; Online Figure IE).

It was previously shown that PE stimulation in neonatal cardiomyocytes resulted in profound AMPK (5’ adenosine monophosphate-activated protein kinase) activation, suggesting the presence of energetic stress after pathological stimuli.[30] However, in ACMs, neither PE stimulation nor ACC2 KD led to activation of AMPK (Online Figure II). Furthermore, there were no changes in cellular ATP levels, indicating that ACM hypertrophy occurred in the absence of any energetic stress (Online Figure IIB). Of note, neither ACC2 KD nor PE stimulation resulted in any change in cellular viability (Online Figure IIC and IID). Thus, we demonstrated that maintenance of FAO during PE stimulation prevents hypertrophic growth of ACMs in an energy-independent manner.

Maintaining FAO Suppresses Glucose Utilization During Hypertrophic Stimulation

We then tested whether elevated FAO in vitro was able to repress glucose utilization. While glucose uptake was increased in ACMs 24 hours after PE stimulation, ACC2 KD robustly attenuated this increase (Figure 2A). Lactate secretion into the culture medium was also lower in ACMs after ACC2 KD and PE stimulation (Figure 2B). Metabolic profiling further confirmed accumulation of glycolytic intermediates in PE-treated ACMs, while this was attenuated after ACC2 KD (Figure 2C; Online Figure IIIA). Together, these data indicate that maintaining FAO prevents the substrate switch and reduces glucose utilization in hypertrophic ACMs in vitro.

To test whether reduction of glucose utilization was causally linked to the antihypertrophic effect of ACC2 deletion, we forced cells to increase glucose usage, by either increasing glucose oxidation (dichloroacetate treatment) or increasing glucose uptake by

overexpression of glucose transporter Glut1 (Figure 2D; Online Figure IIIB). Under both conditions, the antihypertrophic effect of ACC2 KD was reversed, suggesting that the switch toward glucose is key to the hypertrophic growth of ACMs (Figure 2E). Since insulin sensitivity can also affect glucose uptake, we compared hypertrophy of ACMs cultured with or without insulin. The hypertrophic response to PE stimulation was not different when ACMs were cultured insulin-free, neither was the protective effect of ACC2 KD (Online Figure IIIC). This is consistent with prior observations that increased glucose use during pathological hypertrophy is through an insulin-independent mechanism.[31]

To further explore which part of glucose utilization was crucial for the antihypertrophic effect, we replaced glucose by pyruvate, which could directly enter the TCA cycle and bypass glycolysis. While the general hypertrophic response to PE stimulation was not affected, ACC2 KD still effectively prevented cardiomyocyte hypertrophy in the presence of pyruvate (Figure 2F). This suggests that sustained FAO antagonizes glucose utilization downstream of glycolysis.

Sustaining FAO Reduces Aspartate and Nucleotide Levels During Hypertrophic Stimulation

To further explore changes in cellular metabolism, we performed targeted metabolomics by GC/MS and LC/MS (liquid chromatography–mass spectrometry). While TCA cycle intermediates were increased during hypertrophy, ACC2 KD reduced TCA cycle pool size after PE stimulation (Figure 3A and 3B; Online Figure IVA; Online Table I: Metabolite quantification by GC/MS). There was an overall trend toward lower amino acid levels after ACC2 KD (Figure 3A), among which changes in aspartate and glutamine were intriguing. Aspartate levels were increased 2-fold after PE stimulation, and this was attenuated with ACC2 KD/PE. While intracellular glutamine levels did not change after PE stimulation, they were significantly lower after ACC2 KD and ACC2 KD/PE stimulation (Figure 3B). Levels of ribose-5-phosphate were also increased after PE stimulation, indicating activation of the pentose phosphate pathway during hypertrophy. Glutamine, aspartate, and ribose-5-phosphate are required for nucleotide synthesis (Figure 3C).[32] In line with this, levels of purine nucleotides inositol monophosphate, adenosine monophosphate, and guanosine monophosphate were increased after PE stimulation (Figure 3D). After ACC2 KD, both ribose-5-phosphate and purine nucleotide levels were normalized after PE stimulation (Figure 3C and 3D). During de novo purine nucleotide synthesis, fumarate is generated as byproduct.[17,32] Unchanged alpha-ketoglutarate (aKG) and succinate but increased fumarate levels after PE stimulation further support the notion that increased fumarate is not generated through glutamine anaplerosis but as a byproduct of nucleotide synthesis (Online Figure IVA). Together, these data suggest that during ACM hypertrophy, aspartate, glutamine, and ribose-5-phosphate contribute to increased de novo nucleotide synthesis, which is opposed by maintaining FAO.

Preserved FAO Reduces Aspartate Supply for RNA and Protein Synthesis During Hypertrophic Stimulation

As DNA synthesis is low in the heart,[33] we focused on the role of nucleotide supply for RNA and subsequently protein synthesis during ACM growth. RNA and protein synthesis

were significantly increased after PE stimulation in ACMs, and both were attenuated after ACC2 KD (Figure 4A and 4B). To determine whether aspartate availability is limiting for RNA and protein synthesis after ACC2 KD, we treated ACMs with the cell permeable DM-asp. DM-asp supplementation further enhanced RNA and protein synthesis in ACMs stimulated with PE, and it completely reversed the suppression by ACC2 KD (Figure 4A and 4B).

Next, we tested whether increased RNA and protein synthesis by aspartate supplementation were sufficient to restore hypertrophy after ACC2 KD. When ACMs were cultured with DM-asp or in high levels of aspartate, ACC2 KD was unable to protect against cardiomyocyte hypertrophy (Figure 4C; Online Figure VB). Like aspartate, glutamine also contributes to nucleotide synthesis (Figure 3C). Supplementing ACMs with high levels of glutamine or directly providing nucleotide bases also restored hypertrophy after ACC2 KD (Figure 4D). These findings suggest that sustaining FAO primarily restricts the availability of aspartate and glutamine for nucleotide synthesis during PE stimulation. Limiting nucleotide production for RNA synthesis and gene transcription will ultimately reduce protein synthesis and cell growth. Thus, these data collectively suggest that cardiomyocyte hypertrophy requires higher levels of aspartate and glutamine for RNA synthesis.

Next, we wanted to further investigate how sustaining FAO reduced aspartate accumulation and ACM hypertrophy. Importantly, DM-asp supplementation did not affect FAO after ACC2 KD (Online Figure VC), suggesting that the substrate switch drives aspartate accumulation and not the other way around. mTOR (mammalian target of rapamycin) activation has been reported to be sensitive to changes in intracellular metabolite levels.[11,12] However, mTOR and other pro-growth signaling pathways were not affected by DM-asp supplementation and even sustained after ACC2 KD/PE (Online Figures VIA, VIB, and VIIA). This prompted us to look beyond a signaling-based but substrate driven mechanism. As dichloroacetate treatment increased glucose uptake after PE stimulation (Online Figure IIIB) in control and ACC2 KD ACMs, aspartate levels were also increased in both groups after PE stimulation. Pyruvate substitution increased intracellular aspartate levels after PE stimulation in control but not ACC2 KD cells. This observation suggests that the combination of pathological stimuli (PE) and substrate switch toward glucose drives aspartate accumulation to support hypertrophy, supporting the notion that aspartate accumulation is a requirement for ACM hypertrophy (Figure 4E).

Glucose, Not Glutamine, Contributes to Anabolic Aspartate Synthesis During Hypertrophy

Having identified aspartate accumulation as the key contributor to support cardiomyocyte hypertrophy, we next wanted to gain mechanistic insight into its origin. Aspartate can be imported or synthesized through TCA cycle reactions from glucose or glutamine (Figure 5A).[17,34] Aspartate consumption in ACMs was unchanged during PE stimulation and with ACC2 KD (Figure 5B; Online Figure VIIIA). This is consistent with literature showing low uptake of aspartate in most cells[17,34] and suggests that the growth of ACMs during PE stimulation relied on de novo aspartate synthesis. In line with this, ACC2 KD reduced the consumption of glucose and glutamine (Figure 5C; Online Figure VIIIA). To determine the carbon donor for aspartate synthesis, we performed stable isotope tracing with U-^{13}C

glucose and U-^{13}C glutamine to unveil their fate in the TCA cycle and their contribution to aspartate synthesis.

Glutamine enters the TCA cycle through aKG (M+5) after being converted to glutamate (M+5; Figure 5D). aKG can generate aspartate through oxidative (M+4) or reductive (M+3) TCA cycle flux. While 90% of the intracellular glutamine pool was enriched with U-^{13}C glutamine, we found that only 2% to 3% of glutamate or aKG were labeled with ^{13}C, suggesting that glutamine contribution to the TCA cycle is minor in ACMs (Figure 5E). Distinct from proliferating cells, majority of aspartate synthesis in ACMs occurred through oxidative TCA cycle flux (Figure 5F). Importantly, we did not observe any changes in the labeling pattern of TCA cycle intermediates or aspartate after PE stimulation or ACC2 KD (Figure 5E and 5F). These results suggest that glutamine-derived carbons play a minor role in aspartate synthesis during ACM hypertrophy.

Breakdown of glucose during glycolysis gives rise to pyruvate and lactate (Figure 6A). In the mitochondria, pyruvate is oxidized to acetyl-CoA and gives rise to M+2 labeled TCA intermediates, including aspartate (Figure 6A, a). Pyruvate can also enter the TCA cycle through anaplerosis to form oxaloacetate (Figure 6A, b) and generate M+3 citrate or directly form M+3 aspartate. During PE stimulation, we detected increased flux of glucose to lactate, as well as increased contribution of glucose to aspartate synthesis through citrate (M+2) or oxaloacetate (M+3; Figure 6B through 6D). After ACC2 KD, flux of glucose into glycolysis and the TCA cycle was lower, as well as the flux into aspartate (Figure 6B through 6D). Fluxes from glucose into aKG, glutamate, and glutamine were also increased after PE stimulation but lowered with ACC2 KD, suggesting that there was a greater contribution of glucose to the glutamine pool during ACM growth (Figure 6E). Thus, glucose but not glutamine anaplerosis fuels TCA cycle to increase aspartate synthesis during cardiomyocyte growth, which is opposed by preservation of FAO.

To determine whether aspartate acts as a nitrogen donor for nucleotide synthesis during hypertrophy, we added ^{15}N-aspartate to the culture media to label the intracellular aspartate pool and to trace its contribution to purine nucleotides synthesis (Figure 6F). Intracellular aspartate levels were significantly increased during supplementation of aspartate, and ≈60% of the pool was enriched with ^{15}N (Figure 6G). Furthermore, M+1 labeling of adenosine monophosphate was increased after PE stimulation, confirming that aspartate supports nucleotide synthesis as nitrogen donor during hypertrophy (Figure 6H).

Preservation of FAO In Vivo Reduces Glucose-Derived Aspartate Accumulation and Prevents Hypertrophy

We next examined whether preservation of FAO would restrict glucose-derived aspartate synthesis and suppress hypertrophy in vivo. Cardiac-specific ACC2 KO (knockout) mice, which have been shown to maintain FAO during chronic stress,[8,14] were subjected to pressure overload by TAC. Two weeks after TAC, while cardiac systolic function was preserved in control and ACC2 KO mice, significant cardiomyocyte hypertrophy was observed in control but not in ACC2 KO mice (Figure 7A; Online Figure IXA). Metabolite analysis demonstrated a significant increase in aspartate levels in control mice 2 and 4 weeks post-TAC but not in ACC2 KO mice (Figure 7B; Online Figure IXB). Moreover, aspartate

levels correlated with cardiac hypertrophy in WT (wild type) but not in ACC2 KO mice (Online Figure IXC). In vivo stable isotope labeling with U-^{13}C glucose confirmed increased glucose utilization in the TCA cycle (M+2 citrate, glutamate) and a robust synthesis of aspartate (M+2) in control TAC hearts (Figure 7C and 7D). Increased anaplerosis (M+3 citrate, glutamate) also contributed to aspartate synthesis (M+3) in control TAC hearts. In ACC2 KO mice, the contribution of glucose to these pathways remained unchanged after TAC (Figure 7C and 7D), confirming that preservation of FAO during hypertrophic stimulation prevents shuttling of glucose into anabolic substrates such as aspartate in vivo.

In summary, our in vitro and in vivo data collectively show that preservation of FAO during the stimulation of hypertrophy represses upregulation of glucose utilization, specifically, via suppressing the contribution of glucose to the pentose phosphate pathway and through TCA cycle flux into aspartate (Figure 7E).

DISCUSSION

In this study, we demonstrate that preventing the switch of energy substrates in cardiomyocytes during pathological stimulation attenuates the influx of glucose into anabolic precursors and reduces hypertrophic growth in vitro and in vivo. These results advance the field in several aspects: first, we put in place a model of ACMs cultured with multiple substrates. ACMs cultured under these conditions show significant levels of FAO and maintain normal morphology and viability, thus providing a model system for future studies of substrate selection in ACMs. Second, we identify that cellular aspartate accumulation is critical for cardiomyocyte hypertrophy. Third, we show that increased glucose utilization in cardiac hypertrophy supports anabolic metabolism through TCA cycle flux that is antagonized by preserving FAO. As such, our study advances the understanding of the contribution of different substrates to anabolic metabolism and their role in hypertrophic growth and metabolic remodeling.

Current cell culture models have multiple limitations for studying substrate metabolism of cardiomyocytes. Neonatal cardiomyocyte culture is a commonly utilized primary cell model, but the metabolic properties of neonatal cardiomyocytes differ vastly from the adult heart.[35] Furthermore, cardiomyocytes cultured in traditional serum-enriched (fetal bovine serum) medium undergo spontaneous dedifferentiation and hypertrophic growth rendering studies of cardiac hypertrophy impossible.[36] Although serum-free culture conditions are able to maintain the cardiomyocytes quiescent, it fails to represent the robust FA utilization observed in the adult heart.[35] Addition of palmitate—a saturated FA—to cell culture induces cell death within <24 hours, which has been described as lipotoxicity.[37] Supplementing the cell culture medium with a physiological mix of long-chain FAs, as described in the present study, does not affect cell viability or morphology. We also demonstrate that FAs in the medium are taken up by cardiomyocytes and oxidized in the mitochondria, and cardiomyocytes cultured under these conditions are responsive to hypertrophic stimulation and deletion of ACC2. Thus, this culture model is suitable for deciphering the role of substrate selection in cardiomyocyte hypertrophy and furthermore, holds potential for investigating the role of FAO in other cell types and pathological conditions.

Glycolysis is the nodal point of intermediary metabolism. It can directly generate ATP and fuel carbons into the TCA cycle for further oxidation or deliver carbons to various cellular processes through ancillary pathways such as the pentose phosphate pathway or hexosamine biosynthesis pathway.[21,38] Increased glycolysis has been strongly linked to cardiac hypertrophy, as well as an increased flux into ancillary pathways.[39] This study shows that the upregulation of glycolysis and activation of the pentose phosphate pathway during cardiac hypertrophy is antagonized by ACC2 deletion, supporting a direct repressing role of FAO on glycolysis.[40]

Increased aspartate levels and glucose-derived aspartate accumulation during pressure overload has been reported before.[41,42] However, our study clearly advances these reports by showing that both carbon and nitrogen donors are required for nucleotide synthesis during hypertrophy. We demonstrate that aspartate accumulation is a requirement for cardiomyocyte hypertrophy, driven by the pathological substrate switch and hypertrophic stimuli. Increasing aspartate supply is sufficient to reverse the antihypertrophic effect of ACC2 deletion, suggesting that aspartate levels are limiting for nucleotide synthesis for hypertrophic growth.

This finding extends the previous observation in cancer cells and suggests that nucleotide synthesis is likely a target for manipulating the growth of postmitotic cells.[18,19,43] It is also important to note that aspartate supplementation per se is not sufficient to induce cardiomyocyte hypertrophy, as is the switch to enhanced glucose utilization.[9] Only in the presence of a pathological stimuli like PE, this results in hypertrophy. This is consistent with previous reports that metabolic responses act in concert rather than independent of other growth signals.[13] We thus propose a model where aspartate supports anabolic metabolism to increase biomass downstream of pro-growth signals.

Expression of the aspartate/glutamate transporter SLC1A3 is low in most cells and tissues, including the heart,[16,44,45] making endogenous production an important mechanism to supply aspartate. In proliferating cells, aspartate synthesis is highly dependent on glutamine.[18,19] We find that ACMs during hypertrophic growth do not demonstrate glutamine addiction as described in cancer cells. In the heart, glutamine utilization is very low,[46] and carbon-derived glutamine flux into aspartate did not change during hypertrophy. Instead, the contribution of glucose to aspartate synthesis increased significantly in hypertrophied ACMs, suggesting that distinct mechanisms are used to fuel cell growth in proliferating and postmitotic cells.

Cardiac contraction is a highly energy-consuming process.[47] Normal cardiac metabolism allows all substrates to contribute to cardiac energy provision. This metabolic flexibility guarantees optimal energy supply, especially during increased energy demand. A switch from FAs to glucose in hypertrophied hearts, however, promotes the contribution of glucose to anabolic metabolism. Synthesis of amino acids and nucleotides not only consumes glycolytic and TCA cycle intermediates and directs them away from catabolic metabolism (ie, generation of ATP) but also consumes high levels of ATP.[32,48] Thus, the metabolic demand of contraction versus that of growth becomes competitive. Sustaining FAO suppresses the contribution of glucose and limits growth but also allows adequate

metabolic supply for ATP generation. In support of this notion, we found that maintaining FAO improves myocardial energetics and reduces cardiac hypertrophy induced in vivo by pressure overload—a scenario in which the energy demand of the heart is high.[8] Although our study clearly shows that preventing the pathological substrate switch attenuates cardiac hypertrophy, it remains to be determined whether restoring FAO after the onset of hypertrophy will be beneficial.

While it is generally acknowledged that downregulation of PPARα-PGC1α (peroxisome proliferator-activated receptor alpha-peroxisome proliferator-activated receptor gamma coactivator 1-alpha) transcriptional circuit contributes to reduced FAO in cardiac hypertrophy and failure, the upstream mechanism for increased glucose preference is less clear.[49] It has been suggested that increased glucose utilization in hypertrophied hearts is a compensatory response to energy deficit caused by reduced FAO at a time of high energy demand for cardiac contraction.[5,7,20,50] However, the present study demonstrates a reliance on glucose for cardiomyocyte hypertrophy in vitro—a condition where energy requirement for contraction is removed. The observation supports the notion that activation of early-response genes like *c-myc*, *c-jun*, or *lin28a* are likely driving this process.[48,51] The present study thus reveals a critical role of substrate switch for cell growth independent of energy demand.

In conclusion, our data shed new light on the contribution of intermediary metabolism to the hypertrophic growth of the heart. We identify aspartate synthesis as a rate-limiting step and demonstrate distinct mechanisms for aspartate production supporting growth of proliferating and postmitotic cells. These observations also provide potential strategies for reducing cardiac hypertrophy through metabolic intervention.

Nonstandard Abbreviations and Acronyms

Supplementary Material

Refer to Web version on PubMed Central for supplementary material.

Acknowledgments

We thank the members of the Tian Lab for helpful discussion of the study and the Northwest Metabolomics Research Center (University of Washington) for performing metabolomics analysis.

Sources of Funding

This work was supported, in part, by a postdoctoral fellowship from the German Research Foundation RI 2764/1-1 (to J. Ritterhoff), a research grant from Cambridge Isotope Laboratories, Inc (to J. Ritterhoff), the US National Institutes of Health grants HL-129510 and HL-142628 (to R. Tian) and 1S10OD021562-01 (to D. Raftery), an American Heart Association Postdoctoral Fellowship 15POST21620006 (to D. Shao), the American Heart Association Scientist Development Grant 14SDG18590020 (to S.C. Kolwicz), and the American Heart Association Career Development Grant 18CDA34080486 (to D. Shao)

Glossary

ACC2	acetyl-CoA-carboxylase 2
ACM	adult cardiomyocyte

aKG	alpha-ketoglutarate
DM-asp	dimethyl-aspartate
FA	fatty acid
FAO	fatty acid oxidation
glc+FA	glucose+fatty acid
KO	knockout
MCM	MerCreMer
PE	phenylephrine
TAC	transverse aortic constriction
TCA	tricarboxylic acid
WT	wild type

REFERENCES

1. Levy D, Garrison RJ, Savage DD, Kannel WB, Castelli WP. Prognostic implications of echocardiographically determined left ventricular mass in the Framingham Heart Study. N Engl J Med. 1990;322:1561–1566. doi: 10.1056/NEJM199005313222203 [PubMed: 2139921]
2. Schiattarella GG, Hill JA. Inhibition of hypertrophy is a good therapeutic strategy in ventricular pressure overload. Circulation. 2015;131:1435–1447. doi: 10.1161/CIRCULATIONAHA.115.013894 [PubMed: 25901069]
3. Barger PM, Kelly DP. Fatty acid utilization in the hypertrophied and failing heart: molecular regulatory mechanisms. Am J Med Sci. 1999;318:36–42. doi: 10.1097/00000441-199907000-00006 [PubMed: 10408759]
4. Allard MF, Schönekess BO, Henning SL, English DR, Lopaschuk GD. Contribution of oxidative metabolism and glycolysis to ATP production in hypertrophied hearts. Am J Physiol. 1994;267:H742–H750. doi: 10.1152/ajpheart.1994.267.2.H742 [PubMed: 8067430]
5. Ritterhoff J, Tian R. Metabolism in cardiomyopathy: every substrate matters. Cardiovasc Res. 2017;113:411–421. doi: 10.1093/cvr/cvx017 [PubMed: 28395011]
6. Lopaschuk GD, Stanley WC. Malonyl-CoA decarboxylase inhibition as a novel approach to treat ischemic heart disease. Cardiovasc Drugs Ther. 2006;20:433–439. doi: 10.1007/s10557-006-0634-0 [PubMed: 17136490]
7. Luptak I, Balschi JA, Xing Y, Leone TC, Kelly DP, Tian R. Decreased contractile and metabolic reserve in peroxisome proliferator-activated receptor-alpha-null hearts can be rescued by increasing glucose transport and utilization. Circulation. 2005;112:2339–2346. doi: 10.1161/CIRCULATIONAHA.105.534594 [PubMed: 16203912]
8. Kolwicz SC Jr, Olson DP, Marney LC, Garcia-Menendez L, Synovec RE, Tian R. Cardiac-specific deletion of acetyl CoA carboxylase 2 prevents metabolic remodeling during pressure-overload hypertrophy. Circ Res. 2012;111:728–738. doi: 10.1161/CIRCRESAHA.112.268128 [PubMed: 22730442]
9. Liao R, Jain M, Cui L, D'Agostino J, Aiello F, Luptak I, Ngoy S, Mortensen RM, Tian R. Cardiac-specific overexpression of GLUT1 prevents the development of heart failure attributable to pressure overload in mice. Circulation. 2002;106:2125–2131. doi: 10.1161/01.cir.0000034049.61181.f3 [PubMed: 12379584]
10. Pereira RO, Wende AR, Olsen C, Soto J, Rawlings T, Zhu Y, Anderson SM, Abel ED. Inducible overexpression of GLUT1 prevents mitochondrial dysfunction and attenuates structural

remodeling in pressure overload but does not prevent left ventricular dysfunction. J Am Heart Assoc. 2013;2:e000301. doi: 10.1161/JAHA.113.000301 [PubMed: 24052497]

11. Sen S, Kundu BK, Wu HC, Hashmi SS, Guthrie P, Locke LW, Roy RJ, Matherne GP, Berr SS, Terwelp M, et al.Glucose regulation of load-induced mTOR signaling and ER stress in mammalian heart. J Am Heart Assoc. 2013;2:e004796. doi: 10.1161/JAHA.113.004796 [PubMed: 23686371]
12. Sharma S, Guthrie PH, Chan SS, Haq S, Taegtmeyer H. Glucose phosphorylation is required for insulin-dependent mTOR signalling in the heart. Cardiovasc Res. 2007;76:71–80. doi: 10.1016/j.cardiores.2007.05.004 [PubMed: 17553476]
13. Shao D, Villet O, Zhang Z, Choi SW, Yan J, Ritterhoff J, Gu H, Djukovic D, Christodoulou D, Kolwicz SC Jr, et al.Glucose promotes cell growth by suppressing branched-chain amino acid degradation. Nat Commun. 2018;9:2935. doi: 10.1038/s41467-018-05362-7 [PubMed: 30050148]
14. Choi YS, de Mattos AB, Shao D, Li T, Nabben M, Kim M, Wang W, Tian R, Kolwicz SC Jr. Preservation of myocardial fatty acid oxidation prevents diastolic dysfunction in mice subjected to angiotensin II infusion. J Mol Cell Cardiol. 2016;100:64–71. doi: 10.1016/j.yjmcc.2016.09.001 [PubMed: 27693463]
15. Owen OE, Kalhan SC, Hanson RW. The key role of anaplerosis and cataplerosis for citric acid cycle function. J Biol Chem. 2002;277:30409–30412. doi: 10.1074/jbc.R200006200 [PubMed: 12087111]
16. Tajan M, Hock AK, Blagih J, Robertson NA, Labuschagne CF, Kruiswijk F, Humpton TJ, Adams PD, Vousden KH. A role for p53 in the adaptation to glutamine starvation through the expression of SLC1A3. Cell Metab. 2018;28:721–736.e6. doi: 10.1016/j.cmet.2018.07.005 [PubMed: 30122553]
17. Alkan HF, Walter KE, Luengo A, Madreiter-Sokolowski CT, Stryeck S, Lau AN, Al-Zoughbi W, Lewis CA, Thomas CJ, Hoefler G, et al.Cytosolic aspartate availability determines cell survival when glutamine is limiting. Cell Metab. 2018;28:706–720.e6. doi: 10.1016/j.cmet.2018.07.021 [PubMed: 30122555]
18. Sullivan LB, Gui DY, Hosios AM, Bush LN, Freinkman E, Vander Heiden MG. Supporting aspartate biosynthesis is an essential function of respiration in proliferating cells. Cell. 2015;162:552–563. doi: 10.1016/j.cell.2015.07.017 [PubMed: 26232225]
19. Birsoy K, Wang T, Chen WW, Freinkman E, Abu-Remaileh M, Sabatini DM. An essential role of the mitochondrial electron transport chain in cell proliferation is to enable aspartate synthesis. Cell. 2015;162:540–551. doi: 10.1016/j.cell.2015.07.016 [PubMed: 26232224]
20. Neubauer SThe failing heart–an engine out of fuel. N Engl J Med. 2007;356:1140–1151. doi: 10.1056/NEJMra063052 [PubMed: 17360992]
21. Gibb AA, Lorkiewicz PK, Zheng YT, Zhang X, Bhatnagar A, Jones SP, Hill BG. Integration of flux measurements to resolve changes in anabolic and catabolic metabolism in cardiac myocytes. Biochem J. 2017;474:2785–2801. doi: 10.1042/BCJ20170474 [PubMed: 28706006]
22. Olson DP, Pulinilkunnil T, Cline GW, Shulman GI, Lowell BB. Gene knockout of acc2 has little effect on body weight, fat mass, or food intake. Proc Natl Acad Sci U S A. 2010;107:7598–7603. doi: 10.1073/pnas.0913492107 [PubMed: 20368432]
23. Tarnavski O, McMullen JR, Schinke M, Nie Q, Kong S, Izumo S. Mouse cardiac surgery: comprehensive techniques for the generation of mouse models of human diseases and their application for genomic studies. Physiol Genomics. 2004;16:349–360. doi: 10.1152/physiolgenomics.00041.2003 [PubMed: 14679301]
24. Bakrania B, Granger JP, Harmancey R. Methods for the determination of rates of glucose and fatty acid oxidation in the isolated working rat heart. J Vis Exp. 2016. doi: 10.3791/54497
25. He TC, Zhou S, da Costa LT, Yu J, Kinzler KW, Vogelstein B. A simplified system for generating recombinant adenoviruses. Proc Natl Acad Sci U S A. 1998;95:2509–2514. doi: 10.1073/pnas.95.5.2509 [PubMed: 9482916]
26. Louch WE, Sheehan KA, Wolska BM. Methods in cardiomyocyte isolation, culture, and gene transfer. J Mol Cell Cardiol. 2011;51:288–298. doi: 10.1016/j.yjmcc.2011.06.012 [PubMed: 21723873]

27. Wang Y, Zhang Y, Ding G, May HI, Xu J, Gillette TG, Wang H, Wang ZV. Temporal dynamics of cardiac hypertrophic growth in response to pressure overload. Am J Physiol Heart Circ Physiol. 2017;313:H1119–H1129. doi: 10.1152/ajpheart.00284.2017 [PubMed: 28822967]
28. Masumura Y, Higo S, Asano Y, Kato H, Yan Y, Ishino S, Tsukamoto O, Kioka H, Hayashi T, Shintani Y, et al.Btg2 is a negative regulator of cardiomyocyte hypertrophy through a decrease in cytosolic RNA. Sci Rep. 2016;6:28592. doi: 10.1038/srep28592 [PubMed: 27346836]
29. Chong J, Soufan O, Li C, Caraus I, Li S, Bourque G, Wishart DS, Xia J. MetaboAnalyst 4.0: towards more transparent and integrative metabolomics analysis. Nucleic Acids Res. 2018;46:W486–W494. doi: 10.1093/nar/gky310 [PubMed: 29762782]
30. Chen BL, Ma YD, Meng RS, Xiong ZJ, Wang HN, Zeng JY, Liu C, Dong YG. Activation of AMPK inhibits cardiomyocyte hypertrophy by modulating of the FOXO1/MuRF1 signaling pathway in vitro. Acta Pharmacol Sin. 2010;31:798–804. doi: 10.1038/aps.2010.73 [PubMed: 20581852]
31. Allard MF, Wambolt RB, Longnus SL, Grist M, Lydell CP, Parsons HL, Rodrigues B, Hall JL, Stanley WC, Bondy GP. Hypertrophied rat hearts are less responsive to the metabolic and functional effects of insulin. Am J Physiol Endocrinol Metab. 2000;279:E487–E493. doi: 10.1152/ajpendo.2000.279.3.E487 [PubMed: 10950814]
32. Lane AN, Fan TW. Regulation of mammalian nucleotide metabolism and biosynthesis. Nucleic Acids Res. 2015;43:2466–2485. doi: 10.1093/nar/gkv047 [PubMed: 25628363]
33. Bergmann O, Bhardwaj RD, Bernard S, Zdunek S, Barnabé-Heider F, Walsh S, Zupicich J, Alkass K, Buchholz BA, Druid H, et al.Evidence for cardiomyocyte renewal in humans. Science. 2009;324:98–102. doi: 10.1126/science.1164680 [PubMed: 19342590]
34. Hosios AM, Vander Heiden MG. The redox requirements of proliferating mammalian cells. J Biol Chem. 2018;293:7490–7498. doi: 10.1074/jbc.TM117.000239 [PubMed: 29339555]
35. Lopaschuk GD, Jaswal JS. Energy metabolic phenotype of the cardiomyocyte during development, differentiation, and postnatal maturation. J Cardiovasc Pharmacol. 2010;56:130–140. doi: 10.1097/FJC.0b013e3181e74a14 [PubMed: 20505524]
36. Nippert F, Schreckenberg R, Schluter KD. Isolation and cultivation of adult rat cardiomyocytes. J Vis Exp. 2017. doi: 10.3791/56634
37. H T, B-S FAT JC, B N. Saturated fatty acids induce endoplasmic reticulum stress in primary cardiomyocytes. Endoplasm Reticul Stress Dis. 2015;2015:53–66.
38. Gertz EW, Wisneski JA, Stanley WC, Neese RA. Myocardial substrate utilization during exercise in humans. Dual carbon-labeled carbohydrate isotope experiments. J Clin Invest. 1988;82:2017–2025. doi: 10.1172/JCI113822 [PubMed: 3198763]
39. Meerson FZ, Spiritchev VB, Pshennikova MG, Djachkova LV. The role of the pentose-phosphate pathway in adjustment of the heart to a high load and the development of myocardial hypertrophy. Experientia. 1967;23:530–532. doi: 10.1007/bf02137950 [PubMed: 4228586]
40. Randle PJ. Regulatory interactions between lipids and carbohydrates: the glucose fatty acid cycle after 35 years. Diabetes Metab Rev. 1998;14:263–283. doi: 10.1002/(sici)1099-0895(199812)14:4<263::aid-dmr233>3.0.co;2-c [PubMed: 10095997]
41. Umbarawan Y, Syamsunarno MRAA, Koitabashi N, Yamaguchi A, Hanaoka H, Hishiki T, Nagahata-Naito Y, Obinata H, Sano M, Sunaga H, et al.Glucose is preferentially utilized for biomass synthesis in pressure-overloaded hearts: evidence from fatty acid-binding protein-4 and −5 knockout mice. Cardiovasc Res. 2018;114:1132–1144. doi: 10.1093/cvr/cvy063 [PubMed: 29554241]
42. Sansbury BE, DeMartino AM, Xie Z, Brooks AC, Brainard RE, Watson LJ, DeFilippis AP, Cummins TD, Harbeson MA, Brittian KR, et al.Metabolomic analysis of pressure-overloaded and infarcted mouse hearts. Circ Heart Fail. 2014;7:634–642. doi: 10.1161/CIRCHEARTFAILURE.114.001151 [PubMed: 24762972]
43. Hannan RD, Jenkins A, Jenkins AK, Brandenburger Y. Cardiac hypertrophy: a matter of translation. Clin Exp Pharmacol Physiol. 2003;30:517–527. doi: 10.1046/j.1440-1681.2003.03873.x [PubMed: 12890171]

44. Uhlén M, Fagerberg L, Hallström BM, Lindskog C, Oksvold P, Mardinoglu A, Sivertsson Å, Kampf C, Sjöstedt E, Asplund A, et al.Proteomics. Tissue-based map of the human proteome. Science. 2015;347:1260419. doi: 10.1126/science.1260419 [PubMed: 25613900]
45. The Human Protein Atlas;Protein Atlas version 18.1. www.proteinatlas.org.
46. Lauzier B, Vaillant F, Merlen C, Gélinas R, Bouchard B, Rivard ME, Labarthe F, Dolinsky VW, Dyck JR, Allen BG, et al.Metabolic effects of glutamine on the heart: anaplerosis versus the hexosamine biosynthetic pathway. J Mol Cell Cardiol. 2013;55:92–100. doi: 10.1016/j.yjmcc.2012.11.008 [PubMed: 23201305]
47. Doenst T, Nguyen TD, Abel ED. Cardiac metabolism in heart failure: implications beyond ATP production. Circ Res. 2013;113:709–724. doi: 10.1161/CIRCRESAHA.113.300376 [PubMed: 23989714]
48. Palm W, Thompson CB. Nutrient acquisition strategies of mammalian cells. Nature. 2017;546:234–242. doi: 10.1038/nature22379 [PubMed: 28593971]
49. Duncan JG, Finck BN. The PPARalpha-PGC-1alpha axis controls cardiac energy metabolism in healthy and diseased myocardium. PPAR Res. 2008;2008:253817. doi: 10.1155/2008/253817 [PubMed: 18288281]
50. Tian R, Musi N, D'Agostino J, Hirshman MF, Goodyear LJ. Increased adenosine monophosphate-activated protein kinase activity in rat hearts with pressure-overload hypertrophy. Circulation. 2001;104:1664–1669. doi: 10.1161/hc4001.097183 [PubMed: 11581146]
51. Ma H, Yu S, Liu X, Zhang Y, Fakadej T, Liu Z, Yin C, Shen W, Locasale JW, Taylor JM, et al.Lin28a regulates pathological cardiac hypertrophic growth through Pck2-mediated enhancement of anabolic synthesis. Circulation. 2019;139:1725–1740. doi: 10.1161/CIRCULATIONAHA.118.037803 [PubMed: 30636447]

Novelty and Significance

What Is Known?

- Cardiac pathological hypertrophy is associated with a substrate switch from fatty acid FA oxidation (FAO) to an increased reliance on glucose.
- This leads to impaired cardiac energetics that contributes to cardiac dysfunction but also to adverse remodeling and cardiomyocyte hypertrophy.
- Sustaining FAO in the pressure overloaded heart maintains cardiac function and energetics but also attenuates cardiomyocyte hypertrophy.

What New Information Does This Article Contribute?

- Aspartate is required to drive biomass synthesis during pathological hypertrophy.
- Increased glucose utilization supports aspartate synthesis.
- Preservation of FAO prevents the shift toward anabolic metabolism, thus preventing cardiac hypertrophy.

Cardiac metabolism is optimized to fulfill the high energetic demand of the heart. Altered cardiac substrate metabolism contributes to impaired cardiac energetics and cardiomyocyte hypertrophy during pathological remodeling. Most studies have focused on the role of substrate metabolism for energy provision, but the metabolic requirements that drive cardiomyocyte hypertrophy remain incompletely understood. We show that the switch from FA to glucose is required for anabolic metabolism. Glucose-derived aspartate drives biomass synthesis during pathological hypertrophy. This suggests that the metabolic demand of contraction versus that of growth becomes competitive. Sustaining FAO suppresses the contribution of glucose and limits cardiomyocyte growth but also allows adequate metabolic supply for energy provision. Together, our data uncover a previously unrecognized contribution of glucose metabolism to cellular growth in postmitotic tissue and provide a solid foundation for the development of targeted antihypertrophic interventions.

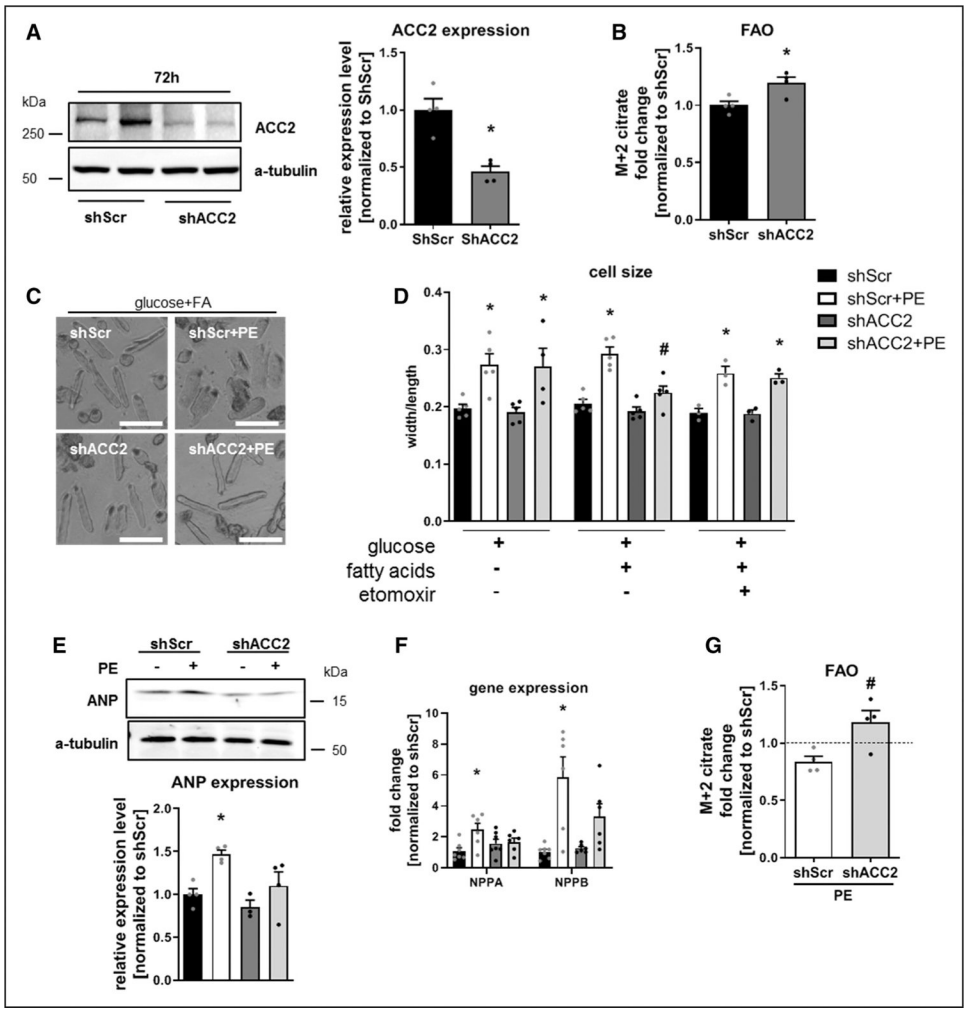

Figure 1. ACC2 (acetyl-CoA-carboxylase 2) KD (knockdown) prevents cardiomyocyte hypertrophy in the presence of fatty acids.

A, Representative immunoblot (**left**) of whole cell lysates and statistical quantification (**right**) of adult cardiomyocyte (ACM) 72 h after adenoviral shRNA knockdown of ACC2. n=4. **B**, Quantification of ^{13}C-fatty acid contribution to M+2 citrate to determine fatty acid oxidation (FAO) in control (shScr) and ACC2 KD (shACC2) CMs. n=4. **C**, Representative images of ACM in glucose+fatty acid (FA) medium with ACC2 KD 24 h after 10 μmol/L phenylephrine (PE) stimulation. Scale bar=100 μm. **D**, Quantification of cell size 24 h after PE stimulation in indicated media. n=3 to 5. **E**, Representative immunoblot (**left**) of whole cell lysates and quantification (**right**) of ANP (atrial natriuretic peptide) protein expression 24 h after PE stimulation. n=4. **F**, Gene expression analysis for hypertrophy markers 24 h after PE stimulation. n=6 to 7. **G**, Quantification of ^{13}C-fatty acid contribution to M+2 citrate to determine FAO 24 h after PE stimulation. The dashed line presents FAO in shScr at baseline. n=4. All data are presented as mean+SEM. *P* values were determined by unpaired Student *t* test (**A** and **B**) or 1-way ANOVA followed by Tukey multiple comparison test (**D**–**G**). **P*<0.05 vs shScr; #*P*<0.05 vs shScr+PE. shACC2 indicates short hairpin RNA against ACC2; and shScr, scrambled short hairpin RNA.

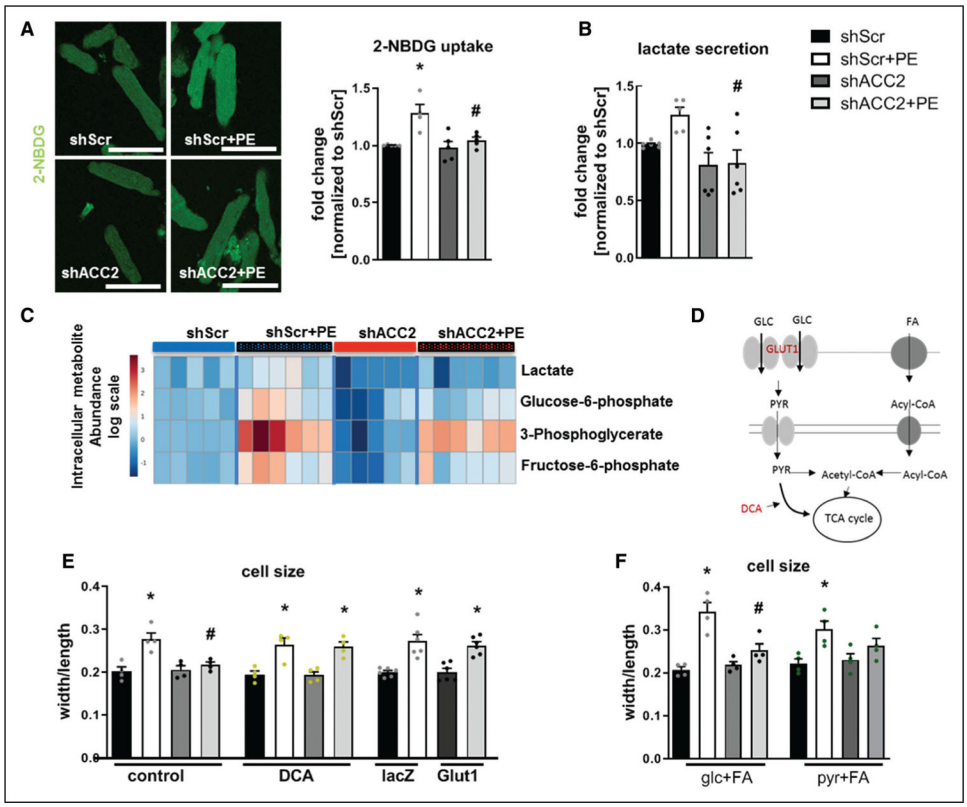

Figure 2. ACC2 (acetyl-CoA-carboxylase 2) KD (knockdown) suppresses glucose utilization and upregulation of glycolysis during hypertrophic stimulation.

A, Representative fluorescent images (**left**) and quantification (**right**) of 2-NBDG uptake 24 h after phenylephrine (PE) stimulation. Scale bar=100 μm. n=4 to 5.**B**, Quantification of lactate secretion into cell culture medium 24 h after PE stimulation. n=5 to 6. **C**, Heat map of glycolytic intermediates 24 h after PE stimulation. n=5. **D**, Schematic depiction of how glucose utilization was increased. **E**, Quantification of cell size 24 h after PE stimulation under indicated conditions. n=5. **F**, Quantification of cell size 24 h after PE stimulation under indicated conditions. n=4. All data are presented as mean+SEM. *P* values were determined by 1-way ANOVA followed by Tukey multiple comparison test. **P*<0.05 vs shScr; #*P*<0.05 vs shScr+PE. shACC2 indicates short hairpin RNA against ACC2; and shScr, scrambled short hairpin RNA.

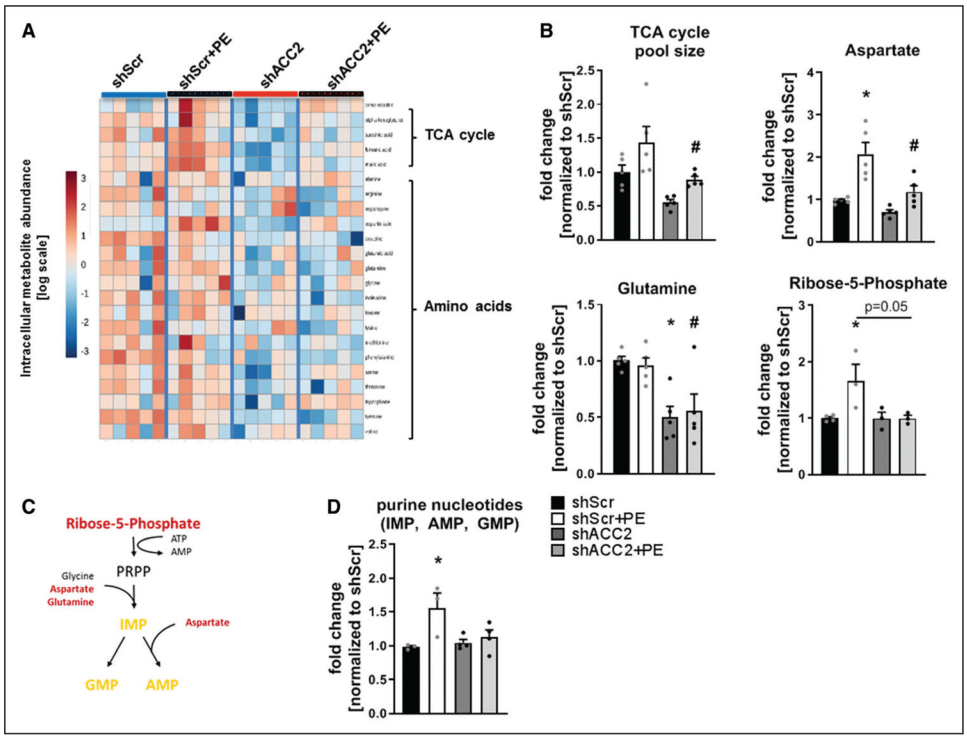

Figure 3. ACC2 (acetyl-CoA-carboxylase 2) KD (knockdown) reduces aspartate and nucleotide levels during hypertrophic stimulation.

A, Heat map depicting tricarboxylic acid (TCA) intermediates and amino acids 24 h after phenylephrine (PE) stimulation (**left**). **B**, Quantification of TCA cycle pool size, intracellular aspartate, glutamine, and ribose-5-phosphate levels. n=3 to 5. **C**, Schematic depiction of how glutamine, aspartate, and ribose-5-phosphate contribute to purine nucleotide generation. **D**, Quantification of purine nucleotides. n=3 to 4. All data are presented as mean+SEM. *P* values were determined by 1-way ANOVA followed by Tukey multiple comparison test. AMP indicates adenosine monophosphate; GMP, guanosine monophosphate; IMP, inositol monophosphate; PRPP, phosphoribosyl pyrophosphate; shACC2, short hairpin RNA against ACC2; and shScr, scrambled short hairpin RNA. **P*<0.05 vs shScr; #*P*<0.05 vs shScr+PE.

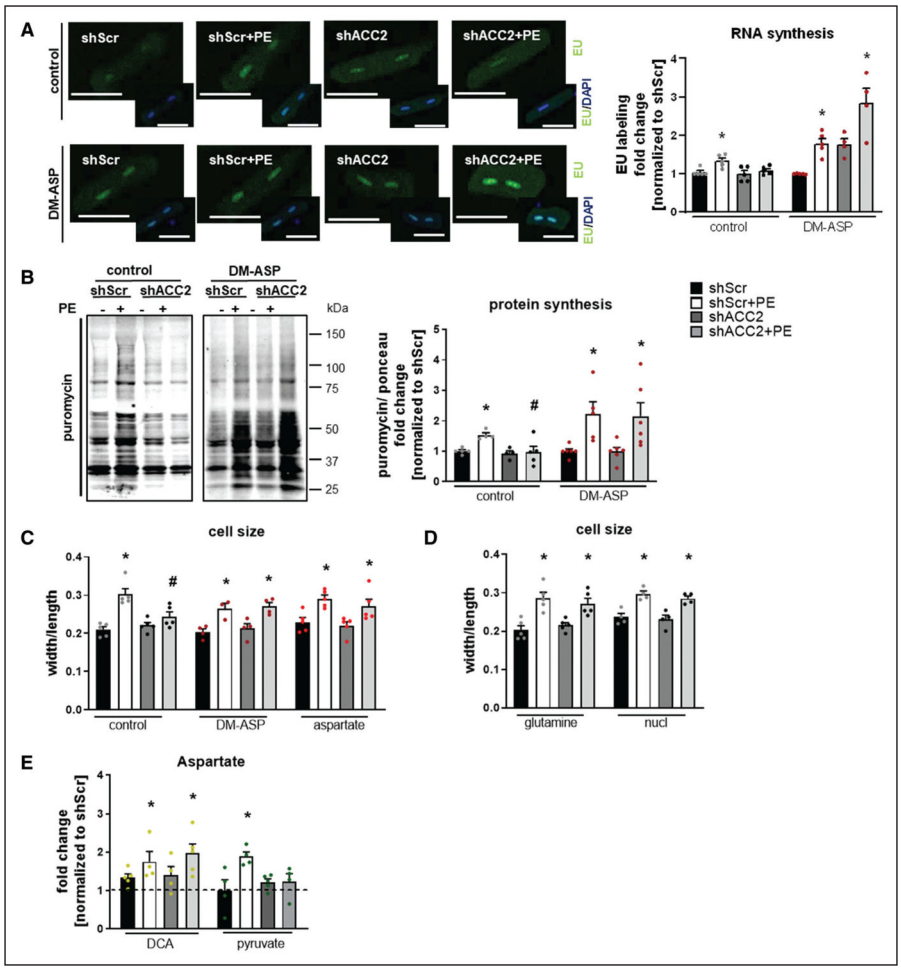

Figure 4. Aspartate supplementation increases RNA and protein synthesis after ACC2 (acetyl-CoA-carboxylase 2) KD (knockdown) during hypertrophy.

A, Representative images (**left**) and quantification (**right**) of RNA synthesis by 5-ethynyl uridine (EU) labeling (green) 22 h after phenylephrine (PE) stimulation in control and dimethyl-aspartate (DM-ASP)–treated CMs. Scale bar =50 μm. n=4 to 5. **B**, Representative image (**left**) and quantification (**right**) of protein synthesis by puromycin incorporation 22 h after PE stimulation in control and DM-ASP–treated CMs. Ponceau loading controls are depicted in the Figure V in the Online Data Supplement. n=4 to 5. **C**, Quantification of cell size 24 h after PE stimulation under indicated conditions. n=4 to 5. **D**, Quantification of cell size 24 h after PE stimulation under indicated conditions. n=4. **E**, Quantification of aspartate levels under indicated conditions (normalized to glucose [glc]+fatty acid [FA] shScr). n=4 to 5. All data are presented as mean+SEM. *P* values were determined by 1-way ANOVA followed by Tukey multiple comparison test. Nucl indicates nucleotides; shACC2, short hairpin RNA against ACC2; and shScr, scrambled short hairpin RNA. **P*<0.05 vs shScr; #*P*<0.05 vs shScr+PE.

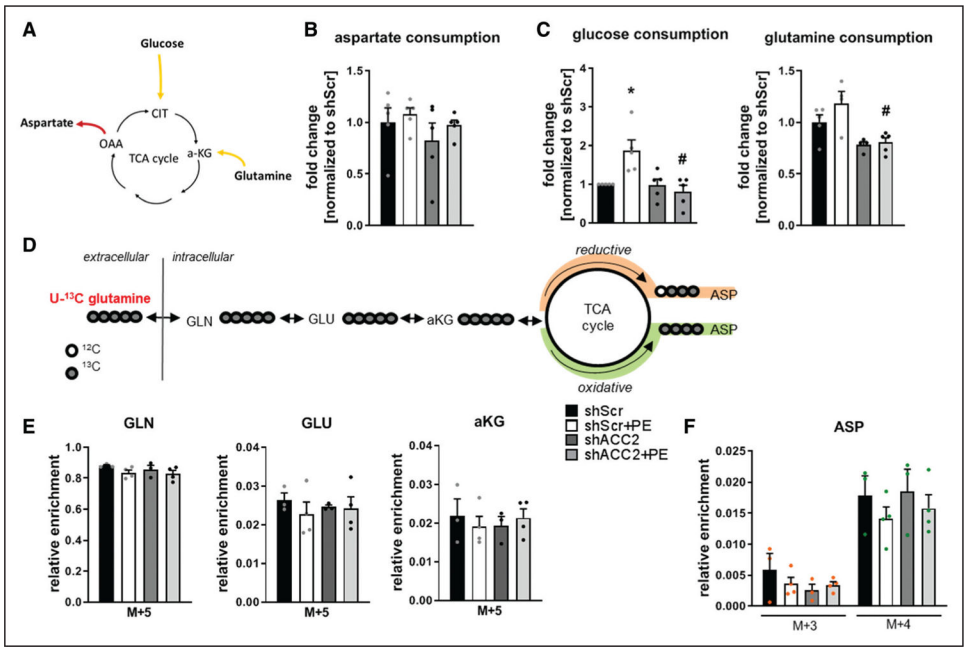

Figure 5. Glutamine (GLN) utilization in tricarboxylic acid (TCA) cycle does not regulate aspartate (ASP) synthesis during hypertrophy.

A, Schematic depiction how glucose and GLN utilization in the TCA cycle support ASP synthesis. **B**, Quantification of ASP consumption from cell culture medium 24 h after phenylephrine (PE) stimulation. n=5. **C**, Quantification of GLN and glucose consumption from cell culture medium 24 h after PE stimulation. n=5. **D**, Schematic depiction of U-^{13}C GLN entry into TCA cycle and labeling pattern of derived metabolites. **E**, Quantification of M+5 GLN, M+5 glutamate (GLU), and M+5 alpha-ketoglutarate (aKG). n=3 to 4. **F**, Quantification of M+3 and M+4 ASP. n=3 to 4. All data are presented as mean+SEM. *P* values were determined by 1-way ANOVA followed by Tukey multiple comparison test. **P*<0.05 vs shScr; #*P*<0.05 vs shScr+PE. shACC2 indicates short hairpin RNA against ACC2; and shScr, scrambled short hairpin RNA.

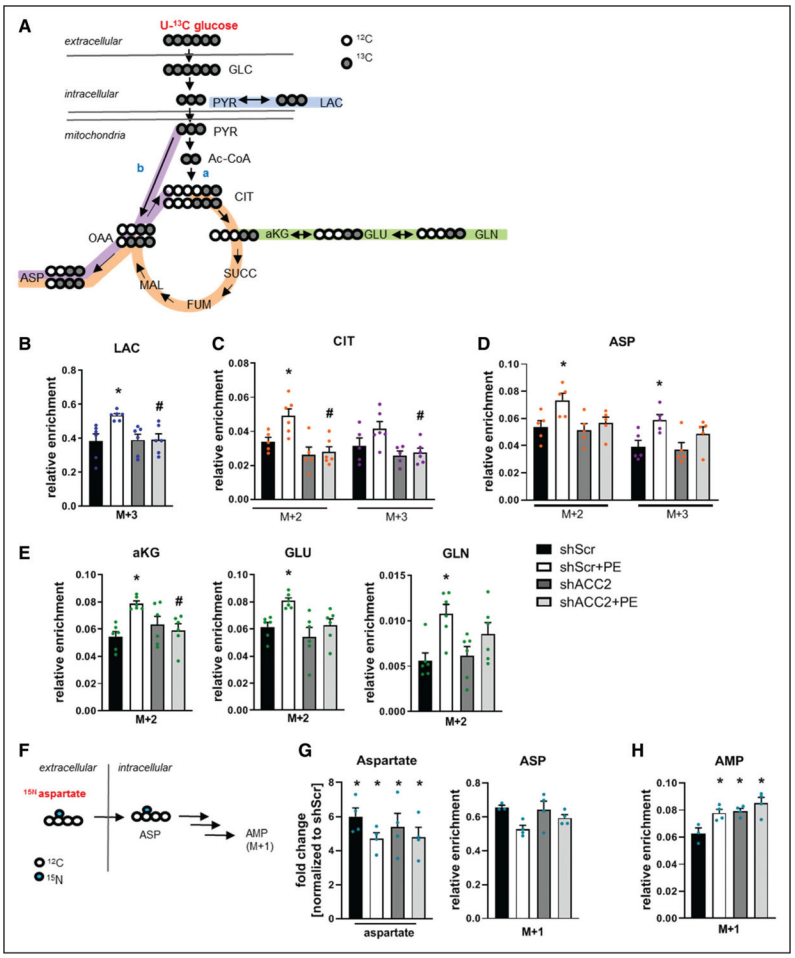

Figure 6. ACC2 (acetyl-CoA-carboxylase 2) KD (knockdown) prevents glucose-derived aspartate (ASP) synthesis in the tricarboxylic acid (TCA) cycle.

A, Schematic depiction of U-^{13}C glucose utilization into TCA cycle and labeling pattern of derived metabolites. **B**, Quantification of M+3 labeling of lactate (LAC). n=6. **C**, Quantification of M+2 and M+3 labeling of citrate (CIT). n=6. **D**, Quantification of M+2 and M+3 labeling of ASP. n=5. **E**, Quantification of M+2 labeling of alpha-ketoglutarate (aKG), glutamate (GLU), and glutamine (GLN). n=6. **F**, Schematic depiction of ^{15}N-aspartate's contribution to adenosine monophosphate (AMP). **G**, Quantification of intracellular ASP levels (normalized to glucose [glc]+fatty acid [FA] shScr, **left**) and M+1 ASP (**right**) after 10 mmol/L ^{15}N-aspartate treatment for 24 h. n=3 to 4. **H**, Quantification of M+1 AMP after ^{15}N-aspartate treatment. n=3 to 4. All data are presented as mean+SEM. *P* values were determined by 1-way ANOVA followed by Tukey multiple comparison test. FUM indicates fumarate; MAL, malate; OAA, oxalacetate; PYR, pyruvate; shACC2, short hairpin RNA against ACC2; shScr, scrambled short hairpin RNA; and SUCC, succinate. **P*<0.05 vs shSCr; #*P*<0.05 vs shScr+phenylephrine (PE).

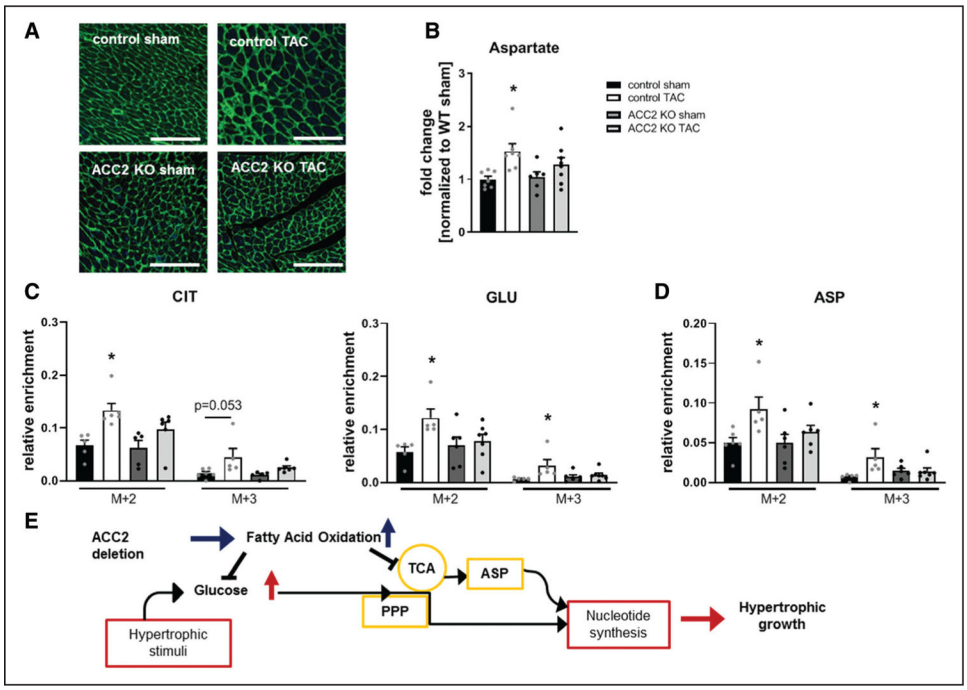

Figure 7. Preservation of fatty acid oxidation (FAO) in vivo reduces glucose-derived aspartate (ASP) synthesis.

A, Representative image of heart sections from ACC2 (acetyl-CoA-carboxylase 2) KO (knockout) and control littermates after sham or transverse aortic constriction (TAC) surgery stained with Wheat Germ Agglutinin (WGA) for cardiac hypertrophy. Scale bar=100 μm. **B**, Quantification for ASP in control and ACC2 KO 2 wk after sham or TAC surgery. n=6 to 8. **C**, Quantification of M+2 and M+3 labeling of citrate (CIT) and glutamate (GLU). n=5 to 6. **D**, Quantification of M+2 and M+3 labeling of ASP. n=5 to 7. **E**, Schematic depiction how FAO prevents CM hypertrophy. All data are presented as mean+SEM. *P* values were determined by 1-way ANOVA followed by Tukey multiple comparison test. PPP indicates pentose phosphate pathway. **P*<0.05 vs control sham; #*P*<0.05 vs WT TAC.